

# Mechanistic Investigation of an Elastically Flexible Organic Crystal

Torvid Feiler, Nobuhiro Yasuda, Adam A. L. Michalchuk,\* Franziska Emmerling,\* and Biswajit Bhattacharya\*



Cite This: *Cryst. Growth Des.* 2023, 23, 6244–6249



Read Online

ACCESS |



Metrics & More

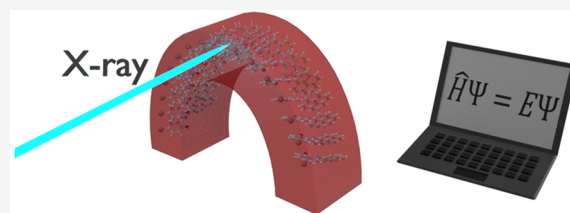


Article Recommendations



Supporting Information

**ABSTRACT:** Mechanical flexibility in molecular crystals is a fascinating behavior with potential for developing advanced technologies. However, the phenomenon of mechanical bending is poorly understood. We explore for the first time the atomistic origin of elastic bending in a single component organic crystal using a combination of  $\mu$ -focus synchrotron X-ray diffraction and *ab initio* simulation.



Mechanically flexible crystals (MFCs) have emerged as a new class of material with exceptional potential for advanced hybrid functionality.<sup>1–9</sup> In this context, mechanical flexibility refers to the ability of a solid to bend under mechanical force, and both terms are used interchangeably. By combining mechanical flexibility with optical and electronic transport properties, shapable nano-optical<sup>10–12</sup> and nano-electronic<sup>13</sup> technologies can be realized without the need to fabricate sophisticated and delicate thin films. Similarly, stimuli responsive MFCs have been proposed for applications in energy harvesting and actuation.<sup>14</sup> Despite the significant technological potential of MFCs, little is known about what structural features give rise to this remarkable mechanical behavior.<sup>15</sup> Correspondingly, new MFCs are generally found serendipitously, precluding the design of hybrid functional materials.

To identify the structural origins of mechanical flexibility, we need to understand how the structure changes as a function of bending. Two approaches are currently being explored. In the first, mechanically flexible crystals are exposed to model stimuli that are believed to induce structural changes akin to bending. Such model stimuli have included studying structural changes as a function of temperature,<sup>16</sup> and as a functional of quasi-hydrostatic compression.<sup>17</sup> Though interesting insights into bending have been made from these model stimuli, there is no guarantee that this indirect information accurately reflects the structural response to bending, often leaving more questions than answers. Alternatively, a growing number of studies have directly probed the structure in bent MFCs, both at the bulk scale by, e.g., mechanical analysis<sup>18</sup> and microscopy,<sup>19</sup> and at the atomic scale by  $\mu$ -focus analyses including Raman spectroscopy and X-ray diffraction.<sup>17,20–22</sup> Coupled with *ab initio* modeling efforts,<sup>17,18,23–26</sup> these studies have revealed exceptional new mechanistic insights into how mechanical flexibility is achieved, pointing toward new material design strategies.

A particularly important feature that has emerged from  $\mu$ -focus structural studies is that the mechanisms of bending can vary for different classes of MFC.<sup>20,22,23,27–29</sup> Whereas mechanical flexibility in coordination polymer crystals can be associated with intertwining of CP chains<sup>18</sup> or distortion of covalent bonds,<sup>19</sup> bending in metal–organic complexes and organic cocrystals occurs through rotation and translation of the discrete complexes about their crystallographic sites.<sup>30</sup> Correspondingly, there is a need to ensure that detailed  $\mu$ -focus structural studies are performed across each class of mechanically flexible crystal to identify when and where mechanistic features are conserved and, more importantly, where they differ. While mechanisms for bending have been studied experimentally for single component elasto-plastic crystals,<sup>23</sup> to the best of our knowledge no experimental studies have been so far reported on the mechanisms of elastic bending in single component organic crystals. To this end, we here report a detailed  $\mu$ -focus structural study on a single component organic MFC, providing the first opportunity to examine the similarities of bending in this class of material as compared with metal–organic complexes and multicomponent crystals.

As model systems, we studied the mechanical bending of two isostructural flexible crystals, *N*-(5-chlorosalicylidene)-1-aminopyrene, *N*-(5-bromosalicylidene)-1-aminopyrene (**Cl-A** and **Br-A**, respectively),<sup>31</sup> Scheme 1. Both compounds were synthesized by liquid-assisted grinding of 1-aminopyrene with the corresponding halo-aldehyde. This was done by grinding an equimolar amount of the starting materials in a mortar and

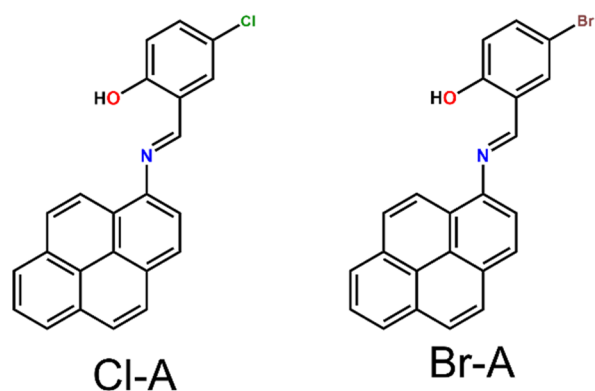
Received: April 18, 2023

Revised: July 26, 2023

Published: August 3, 2023



**Scheme 1. Molecular Structures of Cl-A (*N*-(5-Chlorosalicylidene)-1-aminopyrene) and Br-A (*N*-(5-Bromosalicylidene)-1-aminopyrene)**



pestle and adding a few drops of methanol. For crystallization, the ground powder was dissolved in dichloromethane with ethanol as antisolvent to obtain single crystals (see Supporting Information, Section S1.2).

Both Cl-A, and Br-A crystallize in the orthorhombic space group  $P2_12_12_1$  with one molecule in the asymmetric unit, Table S3.1. All structures are stabilized by intramolecular O–H...N hydrogen bonds (Cl-A,  $d_{\text{H}\cdots\text{N}} = 1.86 \text{ \AA}$ ,  $d_{\text{O}\cdots\text{N}} = 2.60 \text{ \AA}$ ,  $\angle = 146.6^\circ$ , Supporting Information, Figure S3.2, and Br-A,  $d_{\text{H}\cdots\text{N}} = 1.85 \text{ \AA}$ ,  $d_{\text{O}\cdots\text{N}} = 2.60 \text{ \AA}$ ,  $\angle = 147.0^\circ$ , Figure 1) with a slight twisting of the pyrene and phenolic rings with dihedral angles ( $\phi$ ) of  $39.1^\circ$  (Cl-A), and  $39.0^\circ$  (Br-A). In all crystals, the molecules form herringboned chains running along the

crystallographic  $c$ -axis, stabilized by C–H... $\pi$  interactions (Cl-A,  $d_{\text{H}\cdots\pi} = 3.75 \text{ \AA}$ ,  $d_{\text{C}\cdots\pi} = 4.68 \text{ \AA}$ ,  $\angle = 167.3^\circ$ ;  $d_{\text{H}\cdots\pi} = 3.81 \text{ \AA}$ ,  $d_{\text{C}\cdots\pi} = 4.70 \text{ \AA}$ ,  $\angle = 156.2^\circ$ ; Br-A,  $d_{\text{H}\cdots\pi} = 3.82 \text{ \AA}$ ,  $d_{\text{C}\cdots\pi} = 4.75 \text{ \AA}$ ,  $\angle = 166.0^\circ$ ;  $d_{\text{H}\cdots\pi} = 3.88 \text{ \AA}$ ,  $d_{\text{C}\cdots\pi} = 4.77 \text{ \AA}$ ,  $\angle = 157.3^\circ$ ). The chains of Cl-A and Br-A molecules additionally contain C–H...Cl ( $d_{\text{H}\cdots\text{Cl}} = 3.04 \text{ \AA}$ ,  $d_{\text{C}\cdots\text{Cl}} = 3.86 \text{ \AA}$ ,  $\angle = 121.5^\circ$ ) and C–H...Br interactions ( $d_{\text{H}\cdots\text{Br}} = 3.04 \text{ \AA}$ ,  $d_{\text{C}\cdots\text{Br}} = 3.64 \text{ \AA}$ ,  $\angle = 121.8^\circ$ ), respectively (Figure 1 and Figure S3.2). The chains pack in corrugated sheets that sit in the  $bc$ -plane (Figure 1 and Figure S3.2), as is commonly observed for organic crystals with herringboned chains.<sup>24,32</sup> These sheets are slip stacked in a head-to-head manner along the crystallographic  $a$ -axis via  $\pi$ ... $\pi$  interactions (Cl-A,  $3.89 \text{ \AA}$ , Supporting Information, Figure S3.2; Br-A,  $d = 3.92 \text{ \AA}$ , Figure 1). The packing of Cl-A can be found in Supporting Information, Figure S3.2. Face indexing was performed by single crystal X-ray diffraction. The two major faces of Cl-A, and Br-A were identified as being the (010)/ $0\bar{1}0$ ) and (001)/ $00\bar{1}$ ), with the minor face being the (100)/ $\bar{1}00$ ) (Supporting Information, Figure S3.3).

Our energy framework calculations indicate that both crystals exhibit quasi-isotropic intermolecular interactions, Figure 1b, dominated by the  $\pi$ – $\pi$  interactions between herringboned chains along the  $a$ -axis (Cl-A,  $82.5 \text{ kJ mol}^{-1}$ , Supporting Information, Figure S4.1; Br-A,  $83.6 \text{ kJ mol}^{-1}$ , Supporting Information, Figure S4.2). Interactions along the orthogonal crystallographic axes are notably weaker, at  $53.3 \text{ kJ mol}^{-1}/44.9 \text{ kJ mol}^{-1}$  (Cl-A/Br-A) along the  $c$ -axis and  $45.4 \text{ kJ mol}^{-1}/46.0 \text{ kJ mol}^{-1}$  (Cl-A/Br-A) along the  $b$ -axis. Hence, comprising both a herringboned structure and energetically

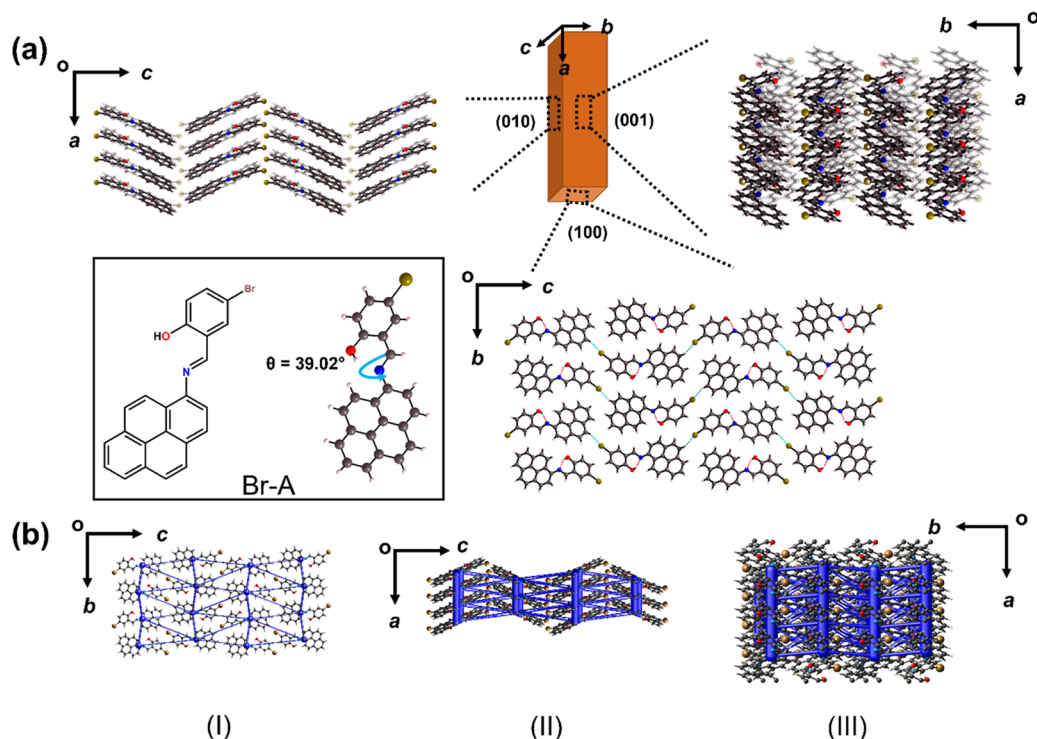


**Figure 1.** Crystallographic structure of MFC Br-A. (a) Crystal packing of Br-A with views along the (001), (100), and (010) faces. The molecular graph and conformation are shown as an inset with the red dotted line indicating the O–H...N interaction ( $1.86 \text{ \AA}$ ). Corresponding figures for the isostructural Cl-A are given in Supporting Information, Figure S3.2. (b) The total intermolecular interaction energy according to the energy framework scheme<sup>33</sup> (blue) shown along the  $a$ -axis (I),  $b$ -axis (II), and  $c$ -axis (III). The line thickness represents the relative magnitude of the interaction energy (minimum energy cutoff  $5 \text{ kJ mol}^{-1}$ ). Full details are given in the Supporting Information, Section S4.2.

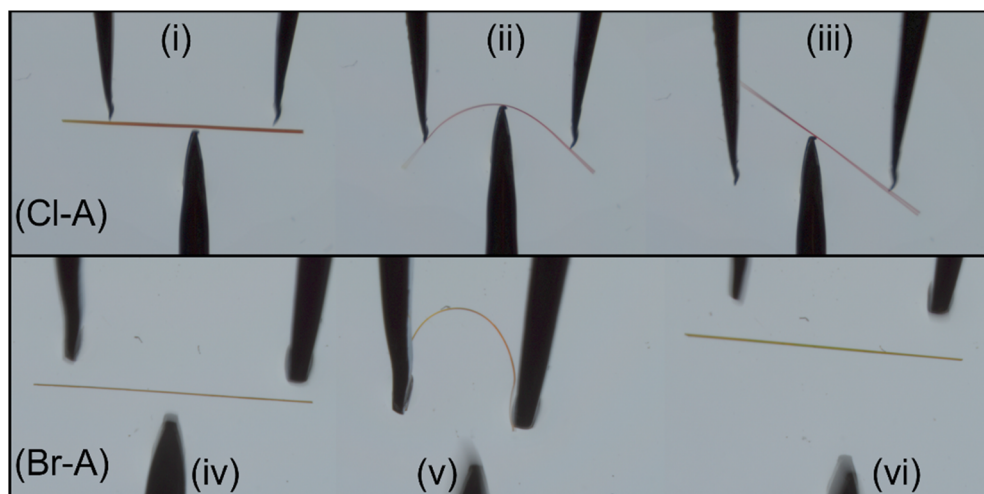


**Figure 2.** Optical microscope photographs of the elastic bending of **CI-A** (i–iii) and **Br-A** (iv–vi) over the crystallographic (001) face.

quasi-isotropic packing, **CI-A** and **Br-A** satisfy the conventional criteria for elastic bending.<sup>34</sup>

The mechanical properties of needle shaped crystals of **CI-A**, and **Br-A** were tested by three-point bending, **Figure 2** and **Figure S5.1**, wherein forceps were used to restrain either end of the crystal while a force was exerted between the forceps by using a needle. Both crystals exhibited a good degree of elasticity when pushed along the (001)/00 $\bar{1}$  face, achieving approximate elastic strains of 1.1% and 1.4% for **CI-A**, and **Br-A**, respectively (Supporting Information, **Figures S5.3** and **S5.4**). These values are comparable with many other elastically flexible molecular crystals.<sup>23,34,35</sup> In contrast, when both the crystals were stressed along the (010)/0 $\bar{1}$ 0 face, brittle fracture was observed (Supporting Information, **Figure S5.2**). In all of the tested crystals, bending could be performed several times without any visible signs of damage or permanent deformation, confirming their macroscopic reversibility.

We sought to identify how bending affects the crystallographic structure by means of  $\mu$ -focus X-ray diffraction (beam size  $0.994 \times 2.76 \mu\text{m}$ ), adopting the data collection strategy suggested elsewhere.<sup>21</sup> As both compounds are isostructural and exhibit the same mechanical behavior, we opted to study only **Br-A** in detail and expect **CI-A** to behave in a similar manner. To study the structure of elastically bent **Br-A**, a single crystal was bent, and both ends were glued to the goniometer needle to maintain the bending during data collection, **Figure 3a** and **Figure S6.1a**. Noticeable anisotropic broadening of Bragg reflections was observed from the scattering of elastically bent crystal. When the crystal returned to its straight form by releasing one end of the crystal from the glue, broadening was lost, thus confirming that data were collected within the elastic regime of the crystal, **Figure 3a–d**. In the bent crystal, the crystallographic  $a$ -axis was found to expand as the probed area approached the convex (outer) face but compress as the concave (inner) face of the bend approached (**Figure 3e**). In contrast, the  $c$ -axis exhibited the opposite trend. This unit cell distortion is consistent with the herringboned layers (in the  $bc$ -plane) being flattened and hence the chains elongating as the herringbone angle increases, **Figure 3e**. Importantly, this structural response is analogous to that observed in our recently reported elastoplastically flexible crystal,<sup>23</sup> indicating that the mechanisms of elasticity are likely conserved within the elastic bending regime of single component molecular

crystals, regardless of the yield limit. However, unlike in the elastoplastic crystals, **Br-A** and **CI-A** do not contain orthogonal slip planes and therefore exhibit purely elastic bending.

The X-ray scattering data for elastically bent **Br-A** were of insufficient quality to solve the atomic structures reliably. We therefore aimed to explore the effects of bending on the crystallographic and molecular structure using DFT calculations following the protocol of our previous investigations.<sup>23,24</sup> To mimic the bent structure, we systematically expanded/compressed the crystallographic  $a$ -axis up to  $\pm 5\%$ , while allowing the rest of the structure to relax under the applied strain, as shown in **Figures 3f** and **3g**. The applied strain exceeds the maximum observed elastic strain of 1.4% to exaggerate the effect on molecular deformation for visibility. In this approach, the outer arc is modeled by the expanded  $a$ -axis while the inner arc is modeled by the contracted  $a$ -axis. Our simulations demonstrate a remarkable qualitative agreement with experimental results, including the discontinuity in the  $c$ -axis response at small deformations of the  $a$ -axis, **Figures 3e** and **3f**. This agreement indicates that our models provide meaningful insight into the effects of bending on **Br-A**.

In the calculated structures, the dihedral angle between pyrene and the phenolic ring increases from the concave (inner) to the convex (outer) face of the bend, **Figure 3g** left. Similarly, the herringbone angle changes considerably with the degree of deformation of the  $a$ -axis, flattening to  $133.66^\circ$  at  $-5\%$  strain (concave surface) and sharpening to  $128.52^\circ$  at  $+5\%$  strain (convex surface), **Figure 3g** right. Bending in **Br-A** is associated with significant energy penalties, as revealed by energy framework calculations, Supporting Information, **Section S8.1**. The expansion of the  $a$ -axis causes the stabilizing  $\pi \cdots \pi$  interactions to weaken by approximately  $7.8 \text{ kJ mol}^{-1}$  for a 5% tensile strain (convex surface), with minimal energy penalties along the  $b$  and  $c$ -axes. In contrast, compression of the  $a$ -axis to 5% compressive strain (concave surface) is associated with a marked stabilization of the cell (ca.  $6.6 \text{ kJ mol}^{-1}$ ). Thus, the sharpening of the herringboned chains may be correlated to softening of the interaction along the  $c$ -axis. DFT calculations, together with energy framework calculations, confirmed our qualitative assessment of structural deformation during bending. DFT calculations allow us to further assume that the flattening of the herringboned chains is accompanied by a sharpening of the dihedral angle.



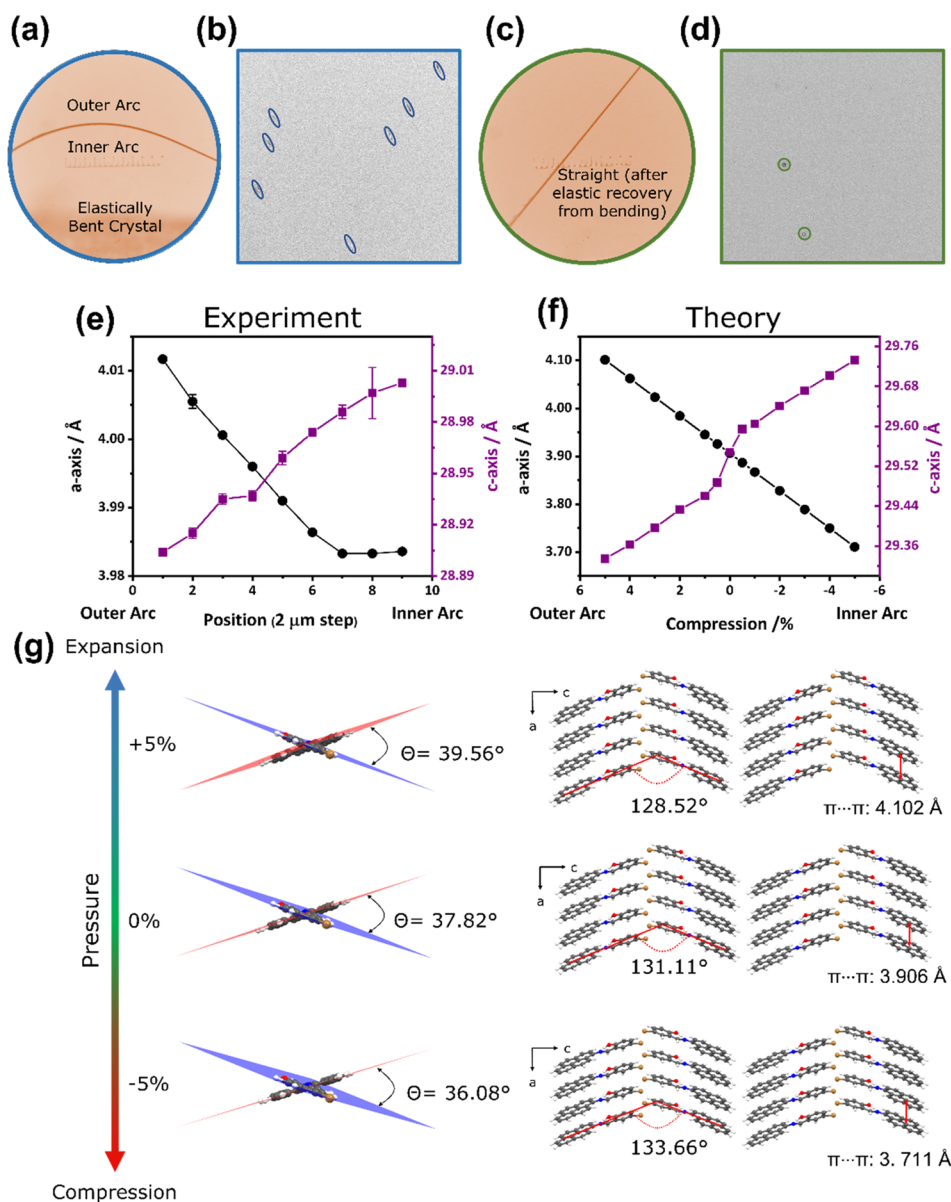


**Figure 3.** Results of -focus X-ray diffraction experiments of mechanically bent single crystals of Br-A. (a) Optical photograph of the elastically bent crystal. (b) The Bragg reflections of the elastic region show notable anisotropic broadening. (c) Optical photograph of the same crystals after releasing of the mechanical force. (d) The sharp Bragg reflection proves a recovery after the bending on the atomistic scale. (e) Nine different positions were measured in the bent crystal. The measurements were taken from the outer ring (position 1) to the inner ring (position 9). The alteration of the unit cell parameters is shown for the *a*-axis (black) and *c*-axis (violet). (f) DFT calculations of uniaxial compression and expansion of the *a*-axis (black) is compared with the response of the *c*-axis (violet) (g) Structural changes upon compression and expansion of the *a*-axis. Left: change in the dihedral angle between pyrene and the phenolic ring. Right: Changes in the  $\pi \cdots \pi$  interaction and flattening of the angle between the herring boned chains.

In summary, we report here the first example of a mechanistic study of an elastically flexible single component organic crystal by combining microfocus X-ray diffraction with *ab initio* simulation. The results indicate that bending is related to expansion/compression of the  $\pi \cdots \pi$  interactions along the crystal axis, which leads to puckering/flattening the herring-boned chains. Importantly, this mechanism is analogous to that observed for the elastic bending of an elastoplastic crystal, suggesting that the mechanism of elastic bending is conserved in single component molecular crystals regardless of the yield limit. Moreover, when compared with mechanistic studies of elastoplastic bending, our results indicate that the lack of a slip plane orthogonal to the herringboned structures offers a design

target to “turn off” elastoplasticity. Our findings therefore demonstrated that the mechanism of elastic bending is conserved in different classes of molecular crystals, while simultaneously offering further insight into material design targets for this fascinating material behavior.

## ASSOCIATED CONTENT

### Supporting Information

The Supporting Information is available free of charge at <https://pubs.acs.org/doi/10.1021/acs.cgd.3c00473>.

Experimental details, computational details, crystallographic information, energy framework calculations,

mechanical properties, synchrotron based microfocus X-ray diffraction, and theoretical calculations (PDF)

Video S1: Elastic bending of Cl-A in (001) face (MP4)

Video S2: Elastic bending of Br-A in (001) face (MP4)

Video S3: Brittle fracture of Cl-A in (010) face (MP4)

Video S4: Brittle fracture of Br-A in (010) face (MP4)

### Accession Codes

CCDC 2247577–2247578 contain the supplementary crystallographic data for this paper. These data can be obtained free of charge via [www.ccdc.cam.ac.uk/data\\_request/cif](http://www.ccdc.cam.ac.uk/data_request/cif), or by emailing [data\\_request@ccdc.cam.ac.uk](mailto:data_request@ccdc.cam.ac.uk), or by contacting The Cambridge Crystallographic Data Centre, 12 Union Road, Cambridge CB2 1EZ, UK; fax: +44 1223 336033.

## AUTHOR INFORMATION

### Corresponding Authors

**Biswajit Bhattacharya** – Department of Materials Chemistry, Federal Institute for Materials Research and Testing (BAM), Berlin 12489, Germany; [orcid.org/0000-0003-4138-1287](https://orcid.org/0000-0003-4138-1287); Email: [biswajit.bhattacharya@bam.de](mailto:biswajit.bhattacharya@bam.de)

**Adam A. L. Michalchuk** – Department of Materials Chemistry, Federal Institute for Materials Research and Testing (BAM), Berlin 12489, Germany; School of Chemistry, University of Birmingham, Birmingham B15 2TT, U.K.; [orcid.org/0000-0001-7405-3269](https://orcid.org/0000-0001-7405-3269); Email: [adam.michalchuk@bam.de](mailto:adam.michalchuk@bam.de), [a.a.l.michalchuk@bham.ac.uk](mailto:a.a.l.michalchuk@bham.ac.uk)

**Franziska Emmerling** – Department of Materials Chemistry, Federal Institute for Materials Research and Testing (BAM), Berlin 12489, Germany; Department of Chemistry, Humboldt-Universität zu Berlin, 12489 Berlin, Germany; [orcid.org/0000-0001-8528-0301](https://orcid.org/0000-0001-8528-0301); Email: [Franziska.emmerling@bam.de](mailto:Franziska.emmerling@bam.de)

### Authors

**Torvid Feiler** – Department of Materials Chemistry, Federal Institute for Materials Research and Testing (BAM), Berlin 12489, Germany; Department of Chemistry, Humboldt-Universität zu Berlin, 12489 Berlin, Germany

**Nobuhiro Yasuda** – Japan Synchrotron Radiation Research Institute (JASRI), Sayo-gun, Hyogo 679-5198, Japan

Complete contact information is available at: <https://pubs.acs.org/10.1021/acs.cgd.3c00473>

### Author Contributions

The manuscript was written through contributions of all authors. All authors have given approval to the final version of the manuscript.

### Funding

B.B. acknowledges funding from Deutsche Forschungsgemeinschaft, Project No. 450137475. The authors thank BAM IT for access to computational resources.  $\mu$ -Focus XRD data were collected at SPring-8 (Japan) under Proposal 2021A1293.

### Notes

The authors declare no competing financial interest.

## REFERENCES

(1) Saha, S.; Mishra, M. K.; Reddy, C. M.; Desiraju, G. R. From Molecules to Interactions to Crystal Engineering: Mechanical Properties of Organic Solids. *Acc. Chem. Res.* **2018**, *51* (11), 2957–2967.

(2) Thompson, A. J.; Chamorro Orué, A. I.; Nair, A. J.; Price, J. R.; McMurtrie, J.; Clegg, J. K. Elastically Flexible Molecular Crystals. *Chem. Rev.* **2021**, *50* (21), 11725–11740.

(3) Hasija, A.; Chopra, D. Potential and Challenges of Engineering Mechanically Flexible Molecular Crystals. *CrystEngComm* **2021**, *23* (34), 5711–5730.

(4) Naumov, P.; Chizhik, S.; Panda, M. K.; Nath, N. K.; Boldyreva, E. Mechanically Responsive Molecular Crystals. *Chem. Rev.* **2015**, *115* (22), 12440–12490.

(5) Reddy, C. M.; Gundakaram, R. C.; Basavoju, S.; Kirchner, M. T.; Padmanabhan, K. A.; Desiraju, G. R. Structural Basis for Bending of Organic Crystals. *Chem. Commun.* **2005**, No. 31, 3945.

(6) Ghosh, S.; Reddy, C. M. Elastic and Bendable Caffeine Cocrystals: Implications for the Design of Flexible Organic Materials. *Angew. Chem., Int. Ed.* **2012**, *51* (41), 10319–10323.

(7) Ghosh, S.; Mishra, M. K. Elastic Molecular Crystals: From Serendipity to Design to Applications. *Cryst. Growth Des.* **2021**, *21* (4), 2566–2580.

(8) Alimi, L. O.; Lama, P.; Smith, V. J.; Barbour, L. J. Hand-Twistable Plastically Deformable Crystals of a Rigid Small Organic Molecule. *Chem. Commun.* **2018**, *54* (24), 2994–2997.

(9) Gupta, P.; Allu, S.; Karothu, D. P.; Panda, T.; Nath, N. K. Organic Molecular Crystals with Dual Stress-Induced Mechanical Response: Elastic and Plastic Flexibility. *Cryst. Growth Des.* **2021**, *21* (4), 1931–1938.

(10) Ravi, J.; Feiler, T.; Mondal, A.; Michalchuk, A. A. L.; Reddy, C. M.; Bhattacharya, B.; Emmerling, F.; Chandrasekar, R. Plastically Bendable Organic Crystals for Monolithic and Hybrid Micro-Optical Circuits. *Adv. Opt. Mater.* **2023**, *11*, 2201518.

(11) Annadhasan, M.; Agrawal, A. R.; Bhunia, S.; Pradeep, V. V.; Zade, S. S.; Reddy, C. M.; Chandrasekar, R. Mechanophotonics: Flexible Single-Crystal Organic Waveguides and Circuits. *Angew. Chem., Int. Ed.* **2020**, *59* (33), 13852–13858.

(12) Annadhasan, M.; Karothu, D. P.; Chinnasamy, R.; Catalano, L.; Ahmed, E.; Ghosh, S.; Naumov, P.; Chandrasekar, R. Micro-manipulation of Mechanically Compliant Organic Single-Crystal Optical Microwaveguides. *Angew. Chem., Int. Ed.* **2020**, *59* (33), 13821–13830.

(13) Yang, X.; Lan, L.; Pan, X.; Liu, X.; Song, Y.; Yang, X.; Dong, Q.; Li, L.; Naumov, P.; Zhang, H. Electrically Conductive Hybrid Organic Crystals as Flexible Optical Waveguides. *Nat. Commun.* **2022**, *13* (1), 7874.

(14) Lan, L.; Yang, X.; Tang, B.; Yu, X.; Liu, X.; Li, L.; Naumov, P.; Zhang, H. Hybrid Elastic Organic Crystals That Respond to Aerial Humidity. *Angew. Chem., Int. Ed.* **2022**, *61* (14), No. e202200196.

(15) Commins, P.; Karothu, D. P.; Naumov, P. Is a Bent Crystal Still a Single Crystal? *Angew. Chem., Int. Ed.* **2019**, *58* (30), 10052–10060.

(16) Rather, S. A.; Saha, B. K. Understanding the Elastic Bending Mechanism in a 9,10-Anthraquinone Crystal through Thermal Expansion Study. *CrystEngComm* **2021**, *23* (34), 5768–5773.

(17) Liu, X.; Michalchuk, A. A. L.; Bhattacharya, B.; Yasuda, N.; Emmerling, F.; Pulham, C. R. High-Pressure Reversibility in a Plastically Flexible Coordination Polymer Crystal. *Nat. Commun.* **2021**, *12* (1), 3871.

(18) Bhattacharya, B.; Michalchuk, A. A. L.; Silbernagl, D.; Rautenberg, M.; Schmid, T.; Feiler, T.; Reimann, K.; Ghalgaoui, A.; Sturm, H.; Paulus, B.; Emmerling, F. A Mechanistic Perspective on Plastically Flexible Coordination Polymers. *Angew. Chem., Int. Ed.* **2020**, *59* (14), 5557–5561.

(19) Pisacić, M.; Biljan, I.; Kodrin, I.; Popov, N.; Soldin, Ž.; Đaković, M. Elucidating the Origins of a Range of Diverse Flexible Responses in Crystalline Coordination Polymers. *Chem. Mater.* **2021**, *33* (10), 3660–3668.

(20) Panda, M. K.; Ghosh, S.; Yasuda, N.; Moriwaki, T.; Mukherjee, G. D.; Reddy, C. M.; Naumov, P. Spatially Resolved Analysis of Short-Range Structure Perturbations in a Plastically Bent Molecular Crystal. *Nature Chem.* **2015**, *7* (1), 65–72.

(21) Thompson, A. J.; Worthy, A.; Grosjean, A.; Price, J. R.; McMurtrie, J. C.; Clegg, J. K. Determining the Mechanisms of

Deformation in Flexible Crystals Using Micro-Focus X-Ray Diffraction. *CrystEngComm* **2021**, *23* (34), 5731–5737.

(22) Worthy, A.; Grosjean, A.; Pfrunder, M. C.; Xu, Y.; Yan, C.; Edwards, G.; Clegg, J. K.; McMurtrie, J. C. Atomic Resolution of Structural Changes in Elastic Crystals of Copper(II) Acetylacetonate. *Nat. Chem.* **2018**, *10* (1), 65–69.

(23) Bhattacharya, B.; Michalchuk, A. A. L.; Silbernagl, D.; Yasuda, N.; Feiler, T.; Sturm, H.; Emmerling, F. An Atomistic Mechanism for Elasto-Plastic Bending in Molecular Crystals. *Chem. Sci.* **2023**, *14* (13), 3441–3450.

(24) Lakshmi pathi, M.; Dey, S.; Emmerling, F.; Bhattacharya, B.; Michalchuk, A. A. L.; Ghosh, S. Designing Dual Mechanical Response in Molecular Crystals through Cocrystallization. *Cryst. Growth Des.* **2022**, *22* (12), 6838–6843.

(25) Ootani, Y.; Kubo, M. Density-Functional Tight-Binding Molecular Dynamics Simulation of the Bending Mechanism of Molecular Crystals. *J. Phys. Chem. C* **2022**, *126* (25), 10554–10565.

(26) Samanta, R.; Das, S.; Mondal, S.; Alkhidir, T.; Mohamed, S.; Senanayak, S. P.; Reddy, C. M. Elastic Organic Semiconducting Single Crystals for Durable All-Flexible Field-Effect Transistors: Insights into the Bending Mechanism. *Chem. Sci.* **2023**, *14* (6), 1363–1371.

(27) Ahmed, E.; Karothu, D. P.; Warren, M.; Naumov, P. Shape-Memory Effects in Molecular Crystals. *Nat. Commun.* **2019**, *10* (1), 3723.

(28) Bhandary, S.; Thompson, A. J.; McMurtrie, J. C.; Clegg, J. K.; Ghosh, P.; Mangalampalli, S. R. N. K.; Takamizawa, S.; Chopra, D. The Mechanism of Bending in a Plastically Flexible Crystal. *Chem. Commun.* **2020**, *56* (84), 12841–12844.

(29) Thomas, S. P.; Shi, M. W.; Koutsantonis, G. A.; Jayatilaka, D.; Edwards, A. J.; Spackman, M. A. The Elusive Structural Origin of Plastic Bending in Dimethyl Sulfone Crystals with Quasi-isotropic Crystal Packing. *Angew. Chem., Int. Ed.* **2017**, *56* (29), 8468–8472.

(30) Brock, A. J.; Whittaker, J. J.; Powell, J. A.; Pfrunder, M. C.; Grosjean, A.; Parsons, S.; McMurtrie, J. C.; Clegg, J. K. Elastically Flexible Crystals Have Disparate Mechanisms of Molecular Movement Induced by Strain and Heat. *Angew. Chem., Int. Ed.* **2018**, *57* (35), 11325–11328.

(31) Safin, D. A.; Bolte, M.; Garcia, Y. Solid-State Photochromism and Thermochromism of N-Salicylidene Pyrene Derivatives. *CrystEngComm* **2014**, *16* (37), 8786.

(32) Feiler, T.; Michalchuk, A. A. L.; Schröder, V.; List-Kratochvil, E.; Emmerling, F.; Bhattacharya, B. Elastic Flexibility in an Optically Active Naphthalidenimine-Based Single Crystal. *Crystals* **2021**, *11* (11), 1397.

(33) Turner, M. J.; Thomas, S. P.; Shi, M. W.; Jayatilaka, D.; Spackman, M. A. Energy Frameworks: Insights into Interaction Anisotropy and the Mechanical Properties of Molecular Crystals. *Chem. Commun.* **2015**, *51* (18), 3735–3738.

(34) Devarapalli, R.; Kadambi, S. B.; Chen, C.-T.; Krishna, G. R.; Kammari, B. R.; Buehler, M. J.; Ramamurty, U.; Reddy, C. M. Remarkably Distinct Mechanical Flexibility in Three Structurally Similar Semiconducting Organic Crystals Studied by Nanoindentation and Molecular Dynamics. *Chem. Mater.* **2019**, *31* (4), 1391–1402.

(35) Mishra, M. K.; Kadambi, S. B.; Ramamurty, U.; Ghosh, S. Elastic Flexibility Tuning via Interaction Factor Modulation in Molecular Crystals. *Chem. Commun.* **2018**, *54* (65), 9047–9050.